Corneal Structural Changes in Nonneoplastic and Neoplastic Monoclonal Gammopathies

Pasquale Aragona,[1] Alessandro Allegra,[2] Elisa Imelde Postorino,[1] Laura Rania,[1] Vanessa Innao,[2] Edward Wylegala,[3] Anna Nowinska,[3] Antonio Ieni,[2] Antonina Pisani,[4] Caterina Musolino,[2] Domenico Puzzolo,[4] and Antonio Micali[4]

[1]Department of Biomedical Sciences, Regional Referral Center for the Ocular Surface Diseases, University of Messina, Messina, Italy
[2]Department of Human Pathology, University of Messina, Messina, Italy
[3]Department of Ophthalmology, District Railway Hospital, Katowice, Poland
[4]Department of Biomedical Sciences, University of Messina, Messina, Italy

Correspondence: Pasquale Aragona, Department of Biomedical Sciences, Regional Referral Center for the Ocular Surface Diseases, University Hospital of Messina, Via Consolare Valeria 1, I-98125, Messina, Italy; paragona@unime.it.

Submitted: November 5, 2015
Accepted: April 3, 2016

Citation: Aragona P, Allegra A, Postorino EI, et al. Corneal structural changes in nonneoplastic and neoplastic monoclonal gammopathies. *Invest Ophthalmol Vis Sci*. 2016;57:2657–2665. DOI:10.1167/iovs.15-18594

Purpose. To investigate corneal confocal microscopic changes in nonneoplastic and neoplastic monoclonal gammopathies.

Methods. Three groups of subjects were considered: group 1, twenty normal subjects; group 2, fifteen patients with monoclonal gammopathy of undetermined significance (MGUS); group 3, eight patients with smoldering multiple myeloma and eight patients with untreated multiple myeloma. After hematologic diagnosis, patients underwent ophthalmologic exam and in vivo confocal microscopic study. The statistical analysis was performed using ANOVA and Student-Newman-Keuls tests and receiver operating characteristic (ROC) curve analysis.

Results. Epithelial cells of gammopathic patients showed significantly higher reflectivity than controls, demonstrated by optical density ($P < 0.001$). Subbasal nerve density, branching, and beading were significantly altered in gammopathic patients ($P = 0.01$, $P = 0.02$, $P = 0.02$, respectively). The number of keratocytes was significantly reduced in neoplastic patients ($P < 0.001$ versus both normal and MGUS) in the anterior, medium, and posterior stroma. The ROC curve analysis showed good sensitivity and specificity for this parameter. Group 2 and 3 keratocytes showed higher nuclear and cytoplasmatic reflectivity in the medium and posterior stroma. Endothelial cells were not affected.

Conclusions. Patients with neoplastic gammopathies showed peculiar alterations of the keratocyte number, which appeared significantly reduced. A follow-up with corneal confocal microscopy of patients with MGUS is suggested as a useful tool to identify peripheral tissue alterations linked to possible neoplastic disease development.

Keywords: gammopathies, in vivo confocal microscopy, cornea, morphometry

Monoclonal gammopathies include a wide group of hematologic conditions, ranging from disorders lacking end-organ damage, such as monoclonal gammopathy of undetermined significance (MGUS) or smoldering multiple myeloma (SMM), to severe life-threatening diseases, such as multiple myeloma (MM).

The International Myeloma Working Group (IMWG), in the diagnostic criteria published in 2010,[1] defined MGUS as a premalignant, asymptomatic, clonal plasma cell proliferation present in more than 3% of the population above the age of 50, characterized by serum M-protein < 3 g/dL, clonal plasma cell population in bone marrow (BM) $< 10\%$, and absence of end-organ damage. Smoldering multiple myeloma is a malignant disease distinguished from MGUS by higher cutoff values (serum M-protein ≥ 3 g/dL and/or clonal plasma cell population in BM $\geq 10\%$), but still lacking end-organ damage. Finally, MM is a malignant plasma cell disorder characterized by excess BM plasma cells, monoclonal protein, osteolytic bone lesions, renal disease, anemia, and hypercalcemia.[1,2]

The eye can be involved in monoclonal gammopathies as a consequence of the ophthalmic localization,[3] blood hyperviscosity,[4,5] or deposition of light chains in the ocular tissues.[6] Among the ocular localizations, corneal involvement is the less well recognized than others.[7] In fact, in gammopathies not accompanied by general symptoms and signs, the diagnosis of primary corneal diseases, such as lattice dystrophy,[8,9] Groenouw type I granular dystrophy,[10] or deep filiform dystrophy,[11] or the diagnosis of systemic diseases such as cystinosis,[12,13] was established.

Corneal transplantation, generally with a good outcome,[14] can be required in the course of gammopathies when severe corneal opacity occurs; however, a recurrence can develop in patients in whom the systemic disease is not controlled by therapy.[15,16]

The corneal lesions occurring in monoclonal gammopathies have been described using in vivo confocal microscopy (IVCM) only in single case reports,[7,13,17–20] examining patients with clinically evident corneal opacities determining alterations of visual acuity. The main confocal features were demonstrated throughout the corneal thickness, showing needle-shaped, hexagonal, or round deposits with crystalline appearance,[7,17,20,21] corresponding on the histopathologic exam to intra- and extracellular tubules, fibrils, and crystals.[9,14,15,22] The lesions occurred either before or after the systemic manifestations of the disease.

The lack of systematic studies describing the corneal changes in patients with clinically defined gammopathy and their possible predictive significance for disease evolution has prompted us to perform for the first time, as far as we know, an analysis of the corneal morphology by IVCM in patients with MGUS, SMM, and MM.

Materials and Methods

Study Design

This cross-sectional study was approved by the Ethics Committee of the University of Messina, Italy, and was conducted in concordance with the tenets of the Declaration of Helsinki. Informed consent was obtained from all the subjects involved in the study after explanation of the nature and possible consequences of the study.

Participants

Thirty-one subjects (18 male, 13 female; age range, 52–84 years; mean age ± standard deviation [SD], 70.9 ± 9.9), recruited at the Department of Human Pathology, Section of Hematology, University of Messina, Messina, Italy, were included in the study. Fifteen (10 males, 5 females; age range, 54–84 years; mean age ± SD, 68.2 ± 11.7 years) were diagnosed as MGUS; 8 (4 males, 4 females; age range, 52–82 years; mean age ± SD, 65 ± 22.6 years) as SMM, and 8 (4 males, 4 females; age range, 64–82 years; mean age, 72 ± 4.8 years) as MM. All patients underwent ophthalmologic examination at the Department of Biomedical Sciences, Regional Referral Center for the Ocular Surface Diseases, University of Messina, Messina, Italy.

Inclusion criteria were the presence of an untreated monoclonal gammopathy documented by hematologic tests and the absence of any corneal opacity evident at the slit-lamp exam.

Exclusion criteria were previous eye injury, infections, trauma, or surgery; presence of corneal alterations unrelated to the gammopathy; and concurrent treatment for the gammopathy.

Furthermore, 20 normal subjects (11 males, 9 females; age range, 42–84 years; mean age ± SD, 63.1 ± 15.4) were recruited at the Department of Biomedical Sciences, Regional Referral Center for the Ocular Surface Diseases, University of Messina, Messina, Italy, to undergo clinical ophthalmologic and hematologic assessment and IVCM study.

The subjects included in the study were divided into three groups: group 1, 20 normal subjects; group 2, 15 MGUS patients; and group 3, 16 neoplastic gammopathic patients (8 SMM and 8 MM).

Hematologic Assessment

The hematologic assessment was carried out on both healthy subjects and patients, including serum immunoglobulin (Ig) A and G classes, lactate dehydrogenase (LDH), and β2-microglobulin, creatinine, and albumin levels. Bone x-ray exam was carried out in all patients. None of the patients was receiving chemotherapy. The degree of disease severity was staged according to the Durie-Salmon staging system and the International Staging System (ISS).[23]

Ophthalmologic Assessment

The ophthalmologic assessment in all subjects was carried out according to the following sequence: best-corrected visual acuity with Early Treatment Diabetic Retinopathy Study (ETDRS) logMAR chart, ocular symptoms questionnaire, slit-lamp evaluation, corneal esthesiometry, IVCM, intraocular pressure (IOP) measurement, and fundus exam.

For the evaluation of symptoms, a visual analogue scale was used for the following symptoms: burning, itching, foreign body sensation, dryness, sticky eye, blurred vision, and photophobia.

Corneoconjunctival fluorescein stain (Bio Glo, fluorescein sodium ophthalmic strips; HUB Pharmaceuticals, LLC, Rancho Cucamonga, CA, USA) was used to identify areas of epithelial damage. The stain was scored according to the NEI/Industry workshop method.[24] The epithelial staining was evaluated with a score from 0 (absent) to 3 (widespread loss of epithelium), with a total score for corneal staining ranging from 0 to 15. A score $\geq$3 was considered abnormal.[25,26]

The corneal sensitivity measurements were performed using the Cochet-Bonnet esthesiometer (Luneau Ophtalmologie, Chartres, France) as previously described.[27]

The IOP was measured using a Goldmann applanation tonometer after topical anesthesia with unpreserved 0.4% oxybuprocaine hydrochloride (Novesina; Novartis Farma, Origgio VA, Italy).

Fundus examination was performed at the slit-lamp, using a Volk +90 D lens (Volk Optical, Mentor, OH, USA).

In Vivo Confocal Microscopy

In vivo confocal microscopy was carried out at least 30 minutes after fluorescein instillation using the Confoscan 4 confocal microscope (Nidek Technologies, Vigonza PD, Italy) following topical instillation of unpreserved 0.4% oxybuprocaine hydrochloride. The examination was performed with the ×40 contact objective, with the additional Z-ring probe to allow precise positioning over the central corneal area. An ophthalmic gel medium (Viscotear; Novartis Farma) was used to improve the adhesion of the lens to the cornea.

A computer-generated code was used to mask the confocal exams so that during image analysis, two experienced observers (PA and DP) were unaware of subjects' name and diagnosis. The images were collected from the central cornea at an illumination intensity set at 76 units and maintained constant for all the exams. A region of interest of 0.1 mm^2 (316 × 316 μm) was considered for each image; the cells overlapping the left and the bottom boundaries were counted, whereas the cells that touched the right and the top boundaries were not included in the evaluation.[28]

Analysis of the IVCM micrographs addressed the following items: epithelial cells, subbasal nerves, number and morphologic features of keratocytes, stromal matrix, and endothelial cell characteristics.

As to the epithelial cells, the IVCM appearance of superficial cells was evaluated to assess the presence of alterations, such as hyperreflectivity of borders and of cytoplasm and/or nuclei.[29–31] For each exam, three well-focused micrographs were randomly selected to evaluate the presence of the above-mentioned alterations, according to the following arbitrary scoring system: 0 = no alterations (no hyperreflective cells); 1 = mild alterations (1–2 cells with hyperreflective cytoplasm per micrograph); 2 = moderate alterations (3–4 cells with hyperreflective cytoplasm or cells with hyperreflective nuclei per micrograph); 3 = severe alterations (more than 4 cells with hyperreflective cytoplasm and/or nuclei or intracellular hyperreflective deposits) (Table 1). Epithelial cell density and area were calculated with the public domain ImageJ software (http://rsb.info.nih.gov/ij/; available in the public domain by the National Institutes of Health, Bethesda, MD, USA) using the function analyze > measure. The epithelial cell area, obtained in square pixels, was converted to μm^2. The epithelial cell

Table 1. Scoring System for In Vivo Confocal Microscopy Parameters

Score	Epithelial Cells	Keratocytes	Stromal Matrix
0	No cells with hyperreflective cytoplasm	No hyperreflective keratocytes	Compact, hyporeflective appearance
1	1–2 cells with hyperreflective cytoplasm	≤4 hyperreflective keratocytes	Coexistence of hyporeflective and hyperreflective areas
2	3–4 cells with hyperreflective cytoplasm or cells with hyperreflective nuclei	5–7 hyperreflective keratocytes	Predominant hyperreflective areas
3	>4 cells with hyperreflective nuclei/cytoplasm or cells with hyperreflective deposits	≥8 hyperreflective keratocytes	Deposits of hyperreflective material

density was expressed as number of cells/mm^2. The optical density (expressed in optical units [OU] from 0 [black] to 255 [white]) of the cells was also calculated using the ImageJ software.

The IVCM nerve analysis was performed on micrographs obtained from the subepithelial layers where the subbasal nerve plexus is present, using the Nerve Analyzer software of the Navis program (Nidek Technologies). The test was carried out on three well-focused micrographs per each corneal scan, as previously reported.[32] In brief, the following parameters of the nerve fibers were considered: density per mm^2, length (μm/mm^2), branching number per mm^2, beading number per mm, beading density per mm^2, and tortuosity according to the Kallinikos index.[33]

As to the keratocytes, the mean number of fully focused cells was considered from anterior, medium, and posterior stroma. To obtain topographic distinction among these sections, all the focused images taken immediately posterior to the subbasal nerve plexus and anterior to the endothelium were considered as stromal limits, and the thickness in between was measured and divided into three parts.[34] The keratocyte density was reported in cells/mm^3, calculating the volume as the selected area of the images multiplied by the ratio between 1 mm and the depth of field of our microscope, equal to 25.4 μm.[28]

Furthermore, the keratocytes' IVCM appearance was evaluated to assess the reflectivity of their bodies as a marker of cellular activity.[35] For each exam, three micrographs from each stromal zone (anterior, medium, and posterior) were selected to evaluate keratocyte morphology according to the following arbitrary scoring system: 0 = no hyperreflective keratocytes per micrograph; 1 = ≤4 hyperreflective keratocytes per micrograph; 2 = 5–7 hyperreflective keratocytes per micrograph; 3 = ≥8 hyperreflective keratocytes per micrograph (Table 1).

As to the analysis of the stromal matrix characteristics, a classification was carried out according to the following arbitrary scoring system based on matrix reflectivity: 0 = compact, hyporeflective appearance; 1 = presence of both hyporeflective and hyperreflective areas; 2 = mainly hyperreflective appearance; 3 = presence of deposits of hyperreflective material (Table 1). The score was obtained from each of three different areas (anterior, medium, and posterior).

For the endothelial cells, the endothelial analyzer software of the Navis program (Nidek Technologies) was used to evaluate their density/mm^2, the mean cellular area expressed in μm^2, the mean number of sides, and the presence of polymegathism and pleomorphism (% of total cells).

Statistical Analysis

The statistical analysis was carried out on the data obtained from 31 patients with gammopathies and 20 normal subjects enrolled at the University of Messina, Messina, Italy.

Primary outcome measures were epithelial morphology, subbasal nerve characteristics, number of hyperreflective keratocytes, and endothelial cell morphology. For the statistical analysis, only data from the right eyes were considered. Analysis of variance was used for comparison among groups; in addition, the Student-Newman-Keuls test was used for pairwise comparisons between groups. Furthermore, receiver operating characteristic (ROC) curve analysis was carried out to identify the specificity and sensitivity of the number of keratocytes among healthy control subjects, MGUS patients, and neoplastic patients. The ROC curve is a useful method to represent the ability of tests or parameters to differentiate between normal and pathologic subjects. In a ROC curve, the true-positive rate (sensitivity) is designed as a function of the false-positive rate (1 − specificity) for different cutoff points of a parameter. The resulting area under the curve (AUC) indicates how well a parameter can distinguish between the examined groups: control or diseased. Classification of area under the curves is reported as <0.7, no discrimination; between 0.7 and 0.8, acceptable discrimination; >0.8, excellent discrimination; and >0.9, outstanding discrimination.[25,36] Spearman's correlation coefficient was calculated between IVCM results and clinical data for MGUS and neoplastic patients.

Values of $P \leq 0.05$ were considered statistically significant. The MedCalc 12.2.1.0 statistical software (MedCalc Software, Ostend, Belgium) was used.

Results

Hematologic Data

None of the healthy subjects showed hematologic changes. Data obtained from both group 2 and 3 patients are shown in Table 2.

Patients with MGUS had a paraprotein class IgG in 14 cases and IgA in one case. Patients with SMM had a paraprotein class IgGκ in three cases, IgGλ in four cases, and IgAκ in one case; BM plasmocytosis was 20 ± 1.4%. MM patients had a paraprotein class IgGλ in three cases and IgGκ in two cases, and a paraprotein class IgAλ in two cases and IgAκ in one case. All MM patients had lytic bone lesions, and BM plasmocytosis was 60.7 ± 20.5%.

Clinical Ophthalmologic Data

The subjects included in the study did not show alteration of visual acuity and did not refer to ocular discomfort symptoms. Furthermore, the slit-lamp exam failed to demonstrate any significant alteration. Corneal sensitivity, IOP, and fundus exam were within normal limits (Table 3).

IVCM Data

The results are presented in Figure 1 and Tables 4 and 5.

In corneal epithelial cells, both group 2 and 3 patients showed a higher reflectivity than controls, as demonstrated by significantly higher optical density values ($P < 0.05$) (Table 4).

The corneal nerve analysis in both group 2 and 3 patients showed increased nerve density and branchings versus control

Investigative Ophthalmology & Visual Science

TABLE 2. Mean Results (±SD) of the Hematologic Data From Group 2 (MGUS) and Group 3 (SMM+MM) Patients

	Number	IgA, g/dL	IgG, g/dL	LDH, U/L	β2-Microglobulin, μg/mL	Creatinine, mg/dL	Albumin, g/dL	No. Patients With Bone Lesions	Bone Marrow Plasmocytosis, %	Stage D-S/ISS
Group 2, MGUS	15	0.64*	1.9 ± 0.4	217 ± 10.2	1.9 ± 0.4	0.9 ± 0.1	4.6 ± 1.2	0/15	Not available	Not applicable
Group 3, SMM+MM	8	1.4*	2.4 ± 1.2	292 ± 18.4	5.3 ± 1.9	1.2 ± 0.4	3.6 ± 0.6	0/8	20 ± 1.4	Not applicable
	8	4.5 ± 1.2	2.3 ± 1.1	246 ± 6.4	4.4 ± 1.7	1.1 ± 0.1	3.5 ± 1.1	8/8	60.7 ± 20.5	5 I A D-S/4 I ISS 1 II A D-S/2 II ISS 2 III A D-S/2 III ISS

D-S, Durie-Salmon staging system.
* Absolute value obtained from one patient.

($P < 0.02$), while group 3 patients demonstrated an increased beading density compared to group 1 subjects ($P < 0.02$) (Table 4).

As to the keratocytes, group 3 patients showed a significantly lower number/mm^3 in the various areas of the stroma (anterior, medium, posterior) ($P < 0.001$) (Table 5).

With regard to keratocyte appearance, it was observed that in the medium and posterior stroma, both group 2 and 3 patients demonstrated a higher reflectivity than group 1 subjects ($P = 0.004$ and $P = 0.001$, respectively) (Table 4).

As to the stromal matrix, it was observed that group 2 and group 3 patients demonstrated a significantly increased reflectivity in the medium stroma as compared to controls ($P = 0.02$) (Table 4).

Taking the number of keratocytes as a marker, the ROC curve analysis for neoplastic and nonneoplastic gammopathies and control subjects showed for the anterior stroma an AUC of 0.989 (95% confidence interval [CI] 0.920–1, $P = 0.0001$), for the medium stroma an AUC of 0.945 (95% CI 0.854–0.987, $P = 0.0001$), and for the posterior stroma an AUC of 0.884 (95% CI 0.775–0.952, $P = 0.0001$). The results are detailed in Figure 2.

The study of the endothelium did not demonstrate any difference among the groups. Furthermore, no correlation was found between IVCM results and clinical data (Supplementary Table).

DISCUSSION

Monoclonal gammopathies may involve the eye because of direct localization of the disease[3] or deposition of light chains in the ocular tissues,[6] or as a consequence of blood hyperviscosity.[4,5] Among the ocular complications, corneal involvement is less well recognized than others.[7] Precise epidemiologic studies on the prevalence of corneal involvement in monoclonal gammopathies are not available; data from Bourne et al.[37] showed a prevalence of one case out of 100 gammopathic patients, while in a prospective study, Aronson and Shaw[38] detected no corneal deposits in 13 patients with MM. These studies referred to the presence of fully developed corneal opacities, clinically evident at the slit-lamp exam and often interfering with patients' sight.

The other papers describing corneal involvement in gammopathies are only single case reports or small case series, referring to fully developed corneal opacities observed either with IVCM or with histopathologic analysis. In a MGUS patient with mild dry eye,[7] all corneal layers were affected by high refractive deposits with crystalline appearance. In particular, the epithelial cells lost their intercellular borders, the anterior stroma showed activated keratocytes, and some crystalline deposits were evident in the endothelial cells. In another MGUS patient,[20] only the basal epithelial cells and the anterior stroma showed highly reflective, granular, and spindle-shaped crystalline deposits, while the subbasal nerves and the endothelium appeared uninvolved. In a SMM patient with bilateral opacities,[19] IVCM demonstrated highly reflective crystalline deposits throughout the corneal layers, with the highest density in the epithelium and anterior stromal keratocytes. Of three single case reports in MM patients,[17,18,20] one described numerous multishaped, discrete, hyperreflective globules randomly distributed within the corneal epithelium and the anterior stroma[17]; the second, numerous hyperreflective needle-shaped structures in the epithelium and stroma[18]; the third, numerous partially hyperreflective crystalline deposits, having a tubular morphology with a central hollow lumen in the corneal epithelium and no deposits in the stroma or in the endothelium.[20]

Table 3. Clinical Data in the Three Groups of Subjects (Controls, MGUS, SMM+MM)

	Symptoms, Score	TBUT, s	Corneal Fluorescein Staining, Score	Corneal Esthesiometry, cm
Group 1, controls	1.8 ± 1.5	8.3 ± 2.2	0.3 ± 0.4	5.9 ± 0.2
Group 2, MGUS	1.6 ± 1.4	7.2 ± 2.8	0.5 ± 0.5	5.9 ± 0.2
Group 3, SMM+MM	1.9 ± 1.6	6.6 ± 1	0.1 ± 0.3	5.9 ± 0.1

TBUT, tear film breakup time expressed in seconds.

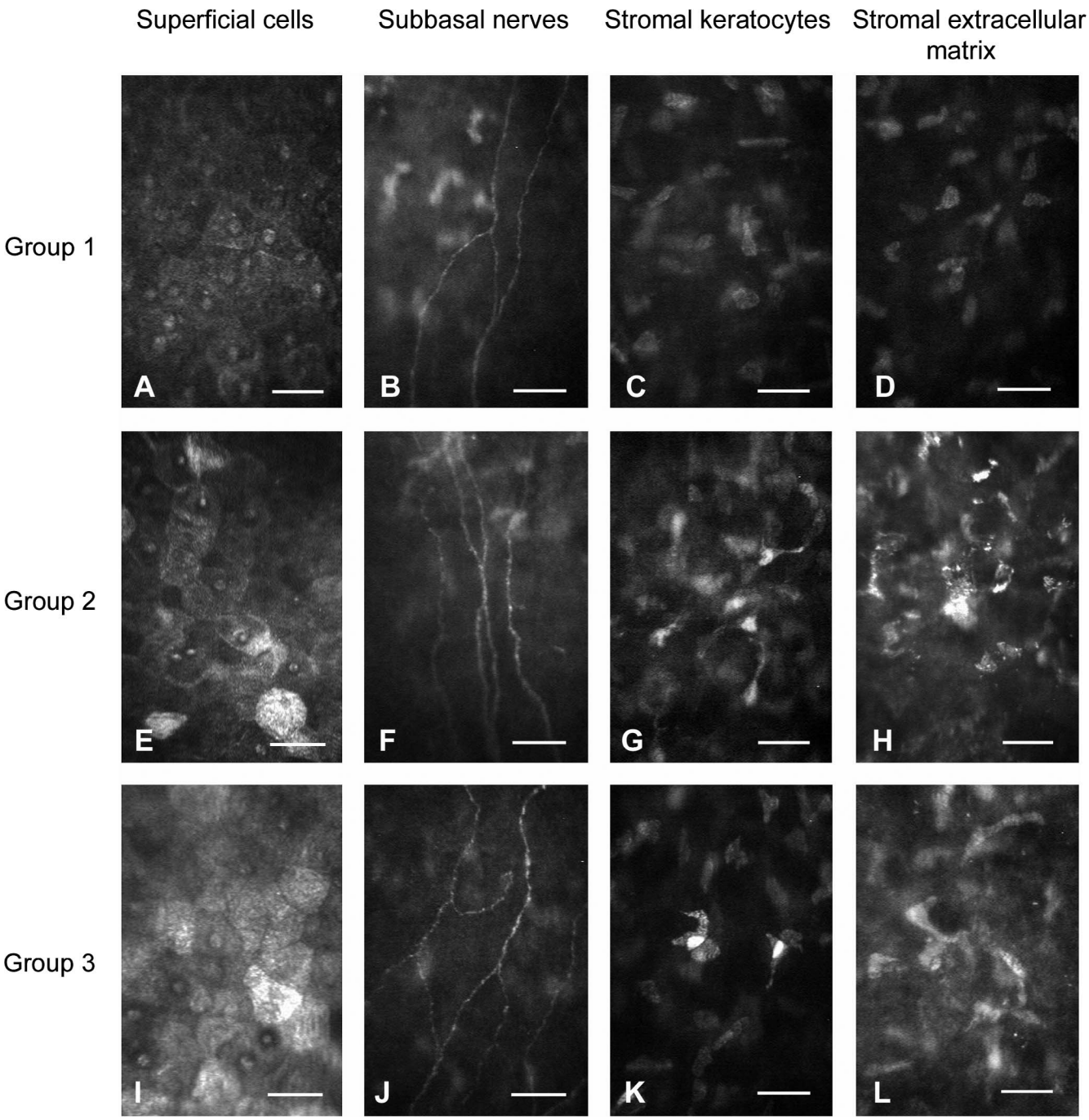

Figure 1. Morphologic patterns of the cornea in groups 1, 2, and 3 obtained with in vivo confocal microscopy. In the epithelium of groups 2 and 3, many superficial cells with higher reflectivity of their cytoplasm were present when compared to controls (**A**, **E**, **I**). The subbasal nerves showed increased density and branching in groups 2 and 3 and an increased amount of beading in group 3 versus control (**B**, **F**, **J**). The keratocytes of both groups 2 and 3 exhibited a higher prevalence of cells with hyperreflective nucleus and cytoplasm than controls (**C**, **G**, **K**). The stromal extracellular matrix showed higher reflectivity in both groups 2 and 3 than in controls (**D**, **H**, **L**). *Scale bars*: 50 μm.

Investigative Ophthalmology & Visual Science

Table 4. Parameter Changes in Group 2, Nonneoplastic Monoclonal Gammopathy of Undetermined Significance, and Group 3, Neoplastic Smoldering and Multiple Myeloma, Versus Group 1 (Healthy Subjects) (for Statistical Analysis the ANOVA Test With the Student-Newman-Keuls Test Was Used)

Parameters	Group 1	Group 2	Group 3
Epithelial cells			
Optical density, 0–255 units	53.8 ± 12.8	68.6 ± 23.1*	72.7 ± 20.4*
Subbasal nerves			
Nerve density, number/mm²	2.5 ± 0.7	4.2 ± 2.5*	4.4 ± 2.3*
Branching, number/mm²	0.6 ± 0.7	1.6 ± 1.7*	1.7 ± 1.3*
Beading density, number/mm²	71.9 ± 14.2	78.9 ± 7.4	82.4 ± 9.2*
Keratocytes			
Score, medium stroma	0.5 ± 0.7	0.9 ± 0.4*	1.2 ± 0.2*
Score, posterior stroma	0.3 ± 0.5	0.9 ± 0.3*	0.8 ± 0.5*
Stromal matrix			
Score, medium stroma	0.9 ± 1.1	1.9 ± 1.1*	1.7 ± 1*

* $P \leq 0.02$ versus group 1.

Table 5. Differences in Keratocyte Number Among Group 2, Nonneoplastic Monoclonal Gammopathy of Undetermined Significance, Group 3, Neoplastic Smoldering and Multiple Myeloma, and Group 1 (Healthy Subjects) (for Statistical Analysis the ANOVA Test With the Student-Newman-Keuls Test Was Used)

Parameters	Group 1	Group 2	Group 3
Keratocytes, number/mm³			
Anterior stroma	30,648 ± 2,934	29,808 ± 3,112	22,581 ± 2,277*
Medium stroma	24,047 ± 2,123	23,700 ± 2,277	18,450 ± 3,049*
Posterior stroma	23,275 ± 2,625	22,813 ± 2,135	19,184 ± 2,663*

* $P < 0.001$ versus group 1 and group 2.

So far, no information is available about possible corneal involvement before a clinically evident opacity occurs. In this respect, the finding of corneal structural changes related to a definite stage of the disease, although not specific to gammopathy, may be of interest for detecting early involvement of the cornea in the disease.

The present study investigated, with IVCM, newly diagnosed, untreated gammopathic patients without a clinically apparent involvement of the cornea. It was carried out on three different populations of gammopathic patients, MGUS, SMM, and MM. While MGUS is a benign condition, SMM and MM are neoplastic diseases[1]; for this reason, in our analysis we allocated SMM and MM neoplastic patients to the same group, comparing the results with those from control and MGUS subjects.

The data obtained demonstrated that the main differences between MGUS subjects and neoplastic patients were in the keratocyte population, which was significantly reduced in all the stromal layers of the neoplastic patient group. Furthermore, in the middle stroma, neoplastic patients demonstrated the highest hyperreflectivity with respect to normals and MGUS patients. Due to the localization of these alterations, the possibility that their presence could be the consequence of concurrent ocular surface disorders, such as dry eye, may be excluded.

Keratocytes are classified via IVCM according to the degree of their reflectivity: Brighter keratocytes are regarded as metabolically active cells,[39] while duller cells are considered to be in a resting condition. This might be in concordance with observations in an electron microscopy study[40] in which bright and dark cells were described according to low or high electron density, corresponding to variations of cellular activity. Therefore, the increased number of hyperreflective keratocytes observed in gammopathic patients might indicate an increased functional activity of the cells,[31] which may lead, in severe cases, to the development of corneal opacification.

The results of the ROC curve analysis demonstrated that keratocyte number could be a good parameter to discriminate between MGUS and neoplastic patients.

Furthermore, the medium and posterior stroma showed an extracellular matrix more reflective in both MGUS and neoplastic patients than in control subjects. This might indicate that, in course of both nonneoplastic and neoplastic gammopathies, a structural rearrangement of the corneal stromal matrix occurs; the increased extracellular reflectivity could be related both to an irregular lamellar arrangement of the collagen, shown histologically in patients with well-evident corneal opacities,[13] or to immunoglobulin deposits shown in corneal opacities by IVCM.[7,21] This feature may resemble those occurring in diseases in which extracellular deposition of abnormal material was demonstrated.[32,41] These stromal changes could be related to abnormal collagen secretion leading to increased stromal density, demonstrated by the brighter appearance at the confocal exam. Such structural modifications might develop into a clinically apparent corneal opacity as demonstrated in patients with severe corneal alterations in the course of gammopathies. The increased activity of keratocytes is a phenomenon common to both MGUS and neoplastic patients. In the latter, higher levels of serum proteins might have a role in the anomalous arrangement of the stromal extracellular matrix, and this might also cause a significant reduction in the number of keratocytes. Different mechanisms have been proposed regarding the ways through which, in myeloma patients, serum proteins reach the cornea. In particular, transport via tear film,[13] diffusion from the aqueous fluid,[15] and increased permeability of the paralimbal vascular arcades[42] have been suggested.

As to the epithelium, the cells showed, in both groups of gammopathic patients, a significantly increased optical density, similar to what has been demonstrated in dry eye.[29,43] This feature could be related to the increased protein content reported in these patients.[1]

The corneal subbasal plexus showed a higher density of beading in neoplastic patients, while both groups of patients had an increased nerve fiber density and branching compared to controls.[34,35] Previously, in gammopathic patients, corneal nerve involvement, consisting of bilateral thickening of the nerve fibers, was shown.[44] On the other hand, the production of TrkA and p75 neurotrophins was demonstrated in B-cell malignancies, including MM, indicating a possible trophic activity on peripheral nerves.[45]

In conclusion, IVCM may bring into evidence differences in gammopathic patients compared with normal controls. Furthermore, the preclinical changes observed in these patients can be considered specific to different stages of the disease. In particular, the number of keratocytes was able to differentiate between MGUS and the neoplastic forms of gammopathy, with good specificity and sensitivity demonstrated in the ROC curve analysis. It should be considered that the results of the present study were obtained using halogen light–based IVCM; therefore, the values obtained for the examined parameters might

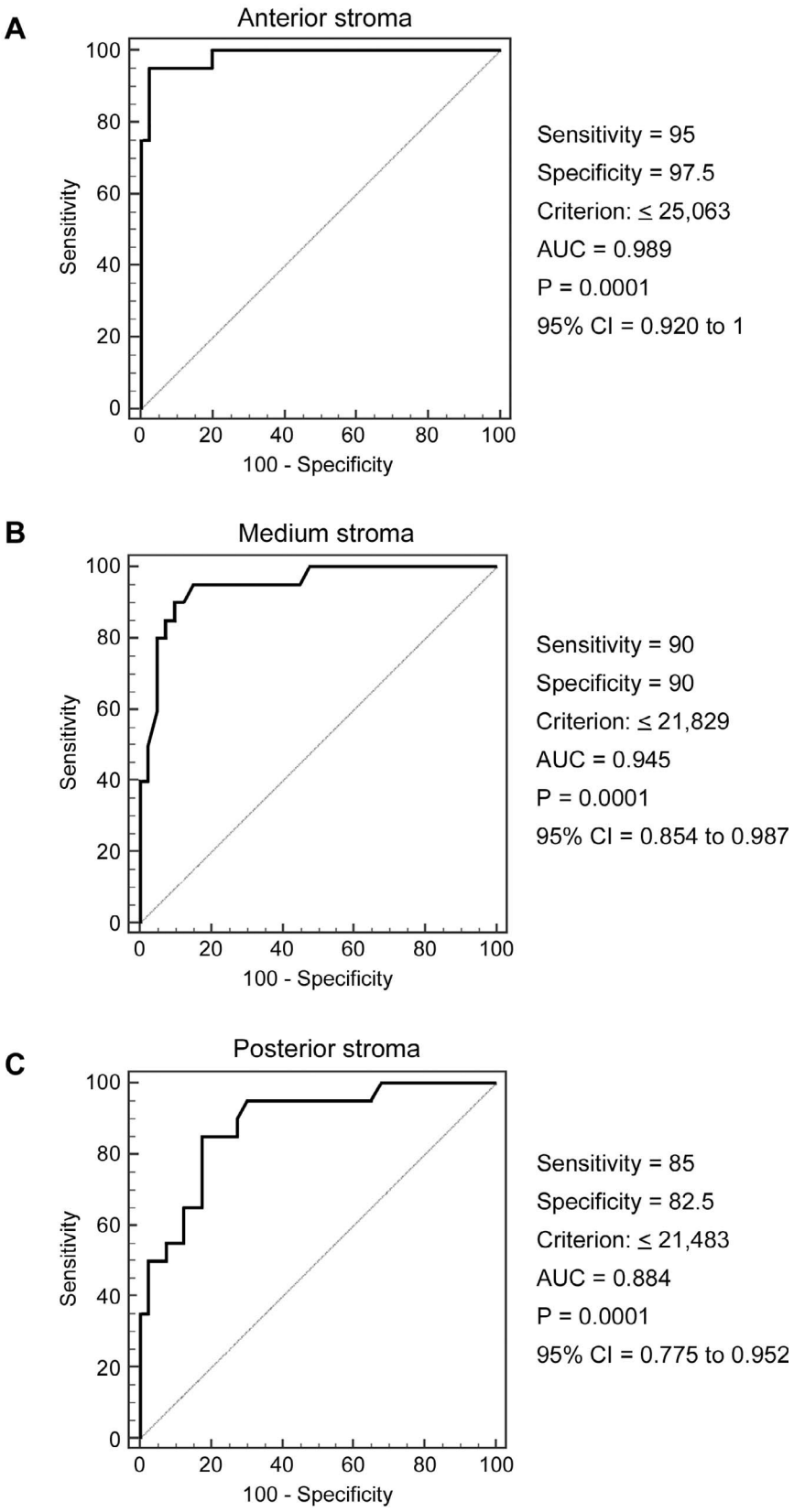

FIGURE 2. Receiver operating characteristic curves for the number of keratocytes in the anterior (**A**), medium (**B**), and posterior (**C**) corneal stroma in healthy control subjects, patients with monoclonal gammopathy of undetermined significance, and patients with smoldering multiple myeloma and multiple myeloma. AUC, area under the receiver operating characteristic curve; CI, confidence interval.

not be superimposable on those from studies using the laser light IVCM. In any case, whatever technology is used, the morphologic differences observed allow one to consider the studied parameters as useful for differentiating between different gammopathic disorders. To confirm such information, a prospective study is necessary; nevertheless, this finding is important as a marker of early structural changes in subjects who might develop relevant corneal opacities.

Improved techniques to risk stratify patients for progression of disease in the course of gammopathic disorders are still lacking. These would be useful for patient counseling and would help in choosing the best follow-up schedule, customized for each patient.

Although gene expression profiling (GEP) has been used to identify molecular signatures associated with different risks of progression from precursor disease to MM,[46] these GEP groups have not yet been validated in an independent cohort of precursor patients and correlated to clinical outcome[47]; corneal IVCM analysis could be a helpful alternative.

Capturing and characterizing early myeloma genesis and identifying patients at high risk of progression are challenges that require further study, and corneal analysis could provide useful information on this topic.

Larger prospective studies could detect corneal pattern heterogeneity in patients with MGUS, enabling prediction of the possible evolution to MM and monitoring of the effects of therapies on peripheral tissues.

Acknowledgments

Disclosure: **P. Aragona**, None; **A. Allegra**, None; **E.I. Postorino**, None; **L. Rania**, None; **V. Innao**, None; **E. Wylegala**, None; **A. Nowinska**, None; **A. Ieni**, None; **A. Pisani**, None; **C. Musolino**, None; **D. Puzzolo**, None; **A. Micali**, None

References

1. Kyle RA, Durie BG, Rajkumar SV, et al.; for International Myeloma Working Group. Monoclonal gammopathy of undetermined significance (MGUS) and smoldering (asymptomatic) multiple myeloma: IMWG consensus perspectives risk factors for progression and guidelines for monitoring and management. *Leukemia*. 2010;24:1121–1127.
2. Raab MS, Podar K, Breitkreutz I, Richardson PG, Anderson KC. Multiple myeloma. *Lancet*. 2009;374:324–339.
3. Chin KJ, Kempin S, Milman T, Finger PT. Ocular manifestations of multiple myeloma: three cases and a review of the literature. *Optometry*. 2011;82:224–230.
4. Fung S, Selva D, Leibovitch I, Hsuan J, Crompton J. Ophthalmic manifestations of multiple myeloma. *Ophthalmologica*. 2005; 219:43–48.
5. Mansour AM, Arevalo JF, Badal J, et al. Paraproteinemic maculopathy. *Ophthalmology*. 2014;121:1925–1932.
6. Sharma P, Madi HA, Bonshek R, Morgan SJ. Cloudy corneas as an initial presentation of multiple myeloma. *Clin Ophthalmol*. 2014;8:813–817.
7. Paladini I, Pieretti G, Giuntoli M, Abbruzzese G, Menchini U, Mencucci R. Crystalline corneal deposits in monoclonal gammopathy: in-vivo confocal microscopy. *Semin Ophthalmol*. 2013;28:37–40.
8. Spiegel P, Grossniklaus HE, Reinhart WJ, Thomas RH. Unusual presentation of paraproteinemic corneal infiltrates. *Cornea*. 1990;9:81–85.
9. Stirling JW, Henderson DW, Rozenbilds MA, Skinner JM, Filipic M. Crystalloidal paraprotein deposits in the cornea: an ultrastructural study of two new cases with tubular crystalloids that contain IgG kappa light chains and IgG gamma heavy chains. *Ultrastruct Pathol*. 1997;21:337–344.
10. Møller HU, Ehlers N, Bojsen-Møller M, Ridgway AE. Differential diagnosis between granular corneal dystrophy Groenouw type I and paraproteinemic crystalline keratopathy. *Acta Ophthalmol (Copenh)*. 1993;71:552–555.
11. Yassa NH, Font RL, Fine BS, Koffler BH. Corneal immunoglobulin deposition in the posterior stroma. A case report including immunohistochemical and ultrastructural observations. *Arch Ophthalmol*. 1987;105:99–103.
12. Kleta R, Blair SC, Bernardini I, Kaiser-Kupfer MI, Gahl WA. Keratopathy of multiple myeloma masquerading as corneal crystals of ocular cystinosis. *Mayo Clin Proc*. 2004;79:410–412.
13. Garibaldi DC, Gottsch J, de la Cruz Z, Haas M, Green WR. Immunotactoid keratopathy: a clinicopathologic case report and a review of reports of corneal involvement in systemic paraproteinemias. *Surv Ophthalmol*. 2005;50:61–80.
14. Steuhl KP, Knorr M, Rohrbach JM, Lisch W, Kaiserling E, Thiel HJ. Paraproteinemic corneal deposits in plasma cell myeloma. *Am J Ophthalmol*. 1991;111:312–318.
15. Ormerod LD, Collin HB, Dohlman CH, Craft JL, Desforges JF, Albert DM. Paraproteinemic crystalline keratopathy. *Ophthalmology*. 1988;95:202–212.
16. Font RL, Matoba AY, Prabhakaran VC. IgG-kappa immunoglobulin deposits involving the predescemetic region in a patient with multiple myeloma. *Cornea*. 2006;25:1237–1239.
17. Buerk BM, Tu E. Confocal microscopy in multiple myeloma crystalline keratopathy. *Cornea*. 2002;21:619–620.
18. Houben N, Foets B. Confocal microscopy in multiple myeloma associated crystalline keratopathy: case report. *Bull Soc Belge Ophthalmol*. 2006;300:13–17.
19. Steinberg J, Eddy MT, Katz T, et al. Bilateral crystalline corneal deposits as first clinical manifestation of monoclonal gammopathy: a case report. *Case Rep Ophthalmol*. 2011;2:222–227.
20. Kocabeyoglu S, Mocan MC, Haznedaroglu IC, Uner A, Uzunosmanoglu E, Irkec M. In vivo confocal microscopic characteristics of crystalline keratopathy in patients with monoclonal gammopathy: report of two cases. *Indian J Ophthalmol*. 2014;62:938–940.
21. Mazzotta C, Caragiuli S, Caporossi A. Confocal microscopy in a case of crystalline keratopathy in a patient with smouldering multiple myeloma. *Int Ophthalmol*. 2014;34:651–654.
22. Henderson DW, Stirling JW, Lipsett J, Rozenbilds MA, Roberts-Thomson PJ, Coster DJ. Paraproteinemic crystalloidal keratopathy: an ultrastructural study of two cases, including immunoelectron microscopy. *Ultrastruct Pathol*. 1993;17: 643–668.
23. Greipp PR, San Miguel J, Durie BG, et al. International staging system for multiple myeloma. *J Clin Oncol*. 2005;23:3412–3420.
24. Lemp MA. Report of the National Eye Institute/Industry Workshop on clinical trials in dry eyes. *CLAO J*. 1995;21: 221–231.
25. Fenga C, Aragona P, Di Nola C, Spinella R. Comparison of ocular surface disease index and tear osmolarity as markers of ocular surface dysfunction in video terminal display workers. *Am J Ophthalmol*. 2014;158:41–48.
26. Aragona P, Aguennouz M, Rania L, et al. Matrix metalloproteinase 9 and transglutaminase 2 expression at the ocular surface in patients with different forms of dry eye disease. *Ophthalmology*. 2015;122:62–71.
27. Aragona P, Tripodi G, Spinella R, Laganà E, Ferreri G. The effects of the topical administration of non-steroidal anti-

inflammatory drugs on corneal epithelium and corneal sensitivity in normal subjects. *Eye*. 2000;14:206–210.

28. McLaren JW, Bourne WM, Patel SV. Automated assessment of keratocyte density in stromal images from ConfoScan 4 confocal microscope. *Invest Ophthalmol Vis Sci*. 2010;51:1918–1926.
29. Chen JJ, Rao K, Pflugfelder SC. Corneal epithelial opacity in dysfunctional tear syndrome. *Am J Ophthalmol*. 2009;148:376–382.
30. Roszkowska AM, Aragona P, Spinella R, Pisani A, Puzzolo D, Micali A. Morphologic and confocal investigation on Salzmann nodular degeneration of the cornea. *Invest Ophthalmol Vis Sci*. 2011;52:5910–5919.
31. Aragona P, Rania L, Roszkowska AM, et al. Effects of amino acids enriched tears substitutes on the cornea of patients with dysfunctional tear syndrome. *Acta Ophthalmol*. 2013;91:437–444.
32. Micali A, Pisani A, Puzzolo D, et al. Macular corneal dystrophy: in vivo confocal and structural data. *Ophthalmology*. 2014;121:1164–1173.
33. Tavakoli M, Kallinikos P, Iqbal A, et al. Corneal confocal microscopy detects improvement in corneal nerve morphology with an improvement in risk factors for diabetic neuropathy. *Diabet Med*. 2011;28:1261–1267.
34. Sturniolo GC, Lazzarini D, Bartolo O, et al. Small fiber peripheral neuropathy in Wilson disease: an in vivo documentation by corneal confocal microscopy. *Invest Ophthalmol Vis Sci*. 2015;56:1390–1395.
35. Chiou AG, Kaufman SC, Kaufman HE, Beuerman RW. Clinical corneal confocal microscopy. *Surv Ophthalmol*. 2006;51:482–500.
36. Hanley JA, McNeil BJ. The meaning and use of the area under a receiver operating characteristic (ROC) curve. *Radiology*. 1982;143:29–36.
37. Bourne WM, Kyle RA, Brubaker RF, Greipp PR. Incidence of corneal crystals in the monoclonal gammopathies. *Am J Ophthalmol*. 1989;107:192–193.
38. Aronson S, Shaw R. Corneal crystals and multiple myeloma. *Arch Ophthalmol*. 1959;61:541–546.
39. Jalbert I, Stapleton F, Papas E, Sweeney DF, Coroneo M. In vivo confocal microscopy of the human cornea. *Br J Ophthalmol*. 2003;87:225–236.
40. Kang GM, Ko MK. Morphological characteristics and intercellular connections of corneal keratocytes. *Korean J Ophthalmol*. 2005;19:213–218.
41. Aragona P, Wylegala E, Wroblewska-Czajka E, et al. Clinical, confocal, and morphological investigations on the cornea in human mucopolysaccharidosis IH-S. *Cornea*. 2014;33:35–42.
42. Schelonka LP, Ogawa GS, O'Brien TP, Green WR. Acute unilateral corneal immunoprotein deposition in IgM monoclonal gammopathy. *Arch Ophthalmol*. 2000;118:125–126.
43. De Paiva CS, Corrales RM, Villarreal AL, et al. Apical corneal barrier disruption in experimental murine dry eye is abrogated by methylprednisolone and doxycycline. *Invest Ophthalmol Vis Sci*. 2006;47:2847–2856.
44. Parghi C, McKnight GT, Pflugfelder SC. Prominent corneal nerves in a patient with multiple myeloma. *Cornea*. 2007;26:220–222.
45. Hillis J, O'Dwyer M, Gorman AM. Neurotrophins and B-cell malignancies. *Cell Mol Life Sci*. 2016;73:41–56.
46. Zhan FH, Barlogie B, John DS Jr. Gene expression profiling defines a high-risk entity of multiple myeloma. *Zhong Nan Da Xue Xue Bao Yi Xue Ban*. 2007;32:191–203.
47. Landgren O. Monoclonal gammopathy of undetermined significance and smoldering multiple myeloma: biological insights and early treatment strategies. *Hematology Am Soc Hematol Educ Program*. 2013;2013:478–487.

Investigative Ophthalmology & Visual Science